A "loss cone" precursor of an approaching shock observed by a cosmic ray muon hodoscope on October 28, 2003

K. Munakata,[1] T. Kuwabara,[1] S. Yasue,[1] C. Kato,[1] S. Akahane,[1] M. Koyama,[1] Y. Ohashi,[2] A. Okada,[2] T. Aoki,[2] K. Mitsui,[3] H. Kojima,[4] and J. W. Bieber[5]

[1] We analyze a loss cone anisotropy observed by a ground-based muon hodoscope at Mt. Norikura in Japan for 7 hours preceding the arrival of an interplanetary shock at Earth on October 28, 2003. Best fitting a model to the observed anisotropy suggests that the loss cone in this event has a rather broad pitch-angle distribution with a half-width about $50°$ from the IMF. According to numerical simulations of high-energy particle transport across the shock, this implies that the shock is a "quasi-parallel" shock in which the angle between the magnetic field and the shock normal is only $6°$. It is also suggested that the lead-time of this precursor is almost independent of the rigidity and about 4 hour at both 30 GV for muon detectors and 10 GV for neutron monitors. **Citation:** Munakata, K., et al. (2005), A "loss cone" precursor of an approaching shock observed by a cosmic ray muon hodoscope on October 28, 2003, *Geophys. Res. Lett.*, *32*, L03S04, doi:10.1029/2004GL021469.

1. Introduction

[2] It is now well established that a coronal mass ejection accompanied by a strong shock often forms a depleted region of galactic cosmic rays behind the shock. A ground-based cosmic ray detector observes a decrease of cosmic ray intensity called a "Forbush Decrease" (FD) when Earth enters the depleted region. A strong enhancement of directional anisotropy of cosmic ray intensity is also associated with a FD. By analyzing the first order anisotropy enhanced during a large FD recorded on October 29, 2003, *Kuwabara et al.* [2004] derived the 3D geometry of the depleted region and compared it with the geometry derived from the magnetic flux rope model.

[3] The enhanced anisotropy is also observed in some events prior to the arrival of the shock at Earth, because cosmic rays travel much faster than the shock and carry the information about the depleted region to Earth far upstream of the approaching shock. The precursory anisotropy is sometimes observed as the "loss cone" (LC) anisotropy, which is characterized by an intensity deficit confined to a narrow pitch angle region around the sunward interplane-

tary magnetic field (IMF) direction [*Munakata et al.*, 2000]. On the basis of numerical simulations of high-energy particle transport across the shock, *Leerungnavarat et al.* [2003] (hereinafter referred to as paper 1) presented the theoretical constraints for LC anisotropy. In the present paper, we analyze a LC precursor observed by a muon hodoscope in operation at Mt. Norikura in Japan and present for the first time a quantitative comparison with theoretical predictions. The muon hodoscope with its excellent angular resolution of the muon incident direction is suitable for measuring a LC anisotropy causing the intensity deficit within a narrow pitch angle region. (It should be noted that the detected muons are secondary particles generated by nuclear interactions of primary cosmic rays with Earth's atmosphere. The primaries are predominantly Galactic cosmic ray protons and helium nuclei.)

2. Observations

[4] A muon hodoscope has been in operation since May 1998 at the top of Mt. Norikura (geographical coordinates are $36.1°N$, $136.6°E$ and the altitude is 2770 m above sea level) in Japan [*Ohashi et al.*, 1997]. It consists of four horizontal layers of 44 proportional counter tubes (PCTs). Each PCT is a 5 m long cylinder with a 10 cm diameter having a 50-micron thick tungsten anode along the cylinder axis. A 5 cm thick lead layer is installed over the top layer to absorb the low energy background radiation in the air. The PCT axis is aligned in the geographical east-west (X) direction in the top and third layers, while the axis is aligned in north-south (Y) direction in the second and bottom layers. The top and second layers touching each other form an upper pair, while the third and bottom layers form a lower pair. These two pairs are vertically separated by 80 cm. The recording of muons is triggered by the four-fold coincidence of pulses from layers and the incident direction of each muon is identified from X-Y locations of hit PCT in each pair. This is approximately equivalent to recording muons with two 44×44 square arrays of 10 cm $\times$ 10 cm detectors vertically separated by 80 cm. For initial performance of this hodoscope, readers can refer to prior publications [*Fujimoto et al.*, 2001, 2003].

[5] We analyze the muon intensity recorded in $11 \times 11 = 121$ directional channels which cover $360°$ of the azimuth angle and $0°$ to $55°$ of the zenith angle. The estimated median energy of primary cosmic rays ranges from 48 GeV for the vertical channel to 80 GeV for the most inclined channel. We first obtain the pressure-corrected hourly count rate in each directional channel, by applying the different correction coefficients for the different zenith angles and thus different atmospheric depths in view. We then normal-
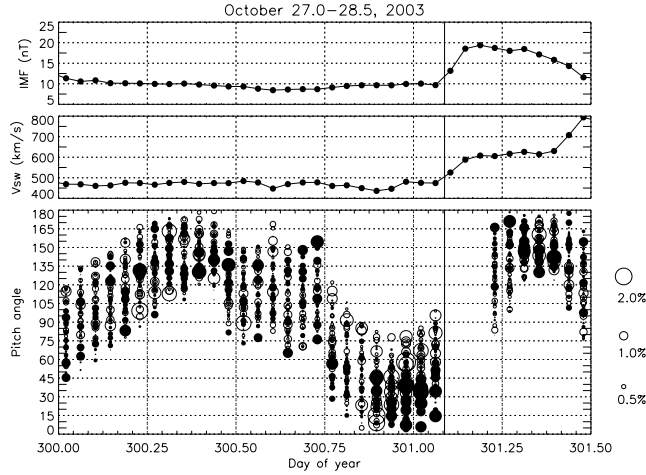
[1]Physics Department, Shinshu University, Matsumoto, Japan.
[2]Institute for Cosmic Ray Research, University of Tokyo, Kashiwa, Japan.
[3]Faculty of Management Information, Yamanashi Gakuin University, Kofu, Japan.
[4]Faculty of Domestic Science, Nagoya Women's University, Nagoya, Japan.
[5]Bartol Research Institute, University of Delaware, Newark, Delaware, USA.

Figure 1. The loss cone precursor observed on October 27–28, 2003. The first and second plots from the top show the 1-hour averages of the IMF magnitude and solar wind speed observed by *ACE* as functions of time (day of year). The increases of IMF magnitude and solar wind velocity indicate the passage of a shock associated with the SSC indicated by the vertical line. In the bottom panel, each circle represents $\Delta I_i^{obs}(t)$ in the *i*-th single directional channel as a function of time *t* (abscissa) and pitch angle (ordinate) of the viewing direction. Open and solid circles represent, respectively, an excess or deficit of intensity relative to the average, and the diameter of each circle is proportional to the magnitude of deficit or excess. To make the LC precursor easy to see, we plotted only data in 61 directional channels (*i* = 1, 3, 5...121) instead of plotting all data in 121 channels.

ize the trailing average of the percent deviation over 24 hours preceding the hour under consideration to that in the vertical channel. This is needed to normalize the data for differing energy responses and suppress the spurious anisotropy sometimes caused by the energy dependent variation in the isotropic component of cosmic ray intensity. We obtain the intensity of muons $\Delta I_i^{obs}(t)$ in the *i*-th directional channel at time *t*(hour) relative to the omnidirectional intensity, as

$$\Delta I_i^{obs}(t) = I_i^{obs}(t) - I^{omni}(t), \quad (1)$$

where $I_i^{obs}(t)$ is the normalized hourly count rate and $I^{omni}(t)$ is defined as

$$I^{omni}(t) = \frac{1}{121} \sum_{i=1}^{121} I_i^{obs}(t). \quad (2)$$

It is noted here that the possible effect of the atmospheric temperature variation is removed from $\Delta I_i^{obs}(t)$ in (1), as the effect is almost common in all directional channels appearing in $I^{omni}(t)$ in (2) [*Sagisaka*, 1986].

[6] Figure 1 shows $\Delta I_i^{obs}(t)$ in each hour as a function of the pitch angle of the incident direction (third plot from the top). In this figure, we calculate the pitch angle using 1-hour averages of the ACE IMF data (level 2), lagged by 1 hour as a rough correction for the solar wind transit time between the ACE satellite and Earth. Seen in this plot is a signature of LC precursor which is displayed as intense deficits (solid

circles) localized around 0° pitch angle during ~7 hours prior to the shock arrival at the time of a Storm Sudden Commencement (SSC) indicated by a vertical line.
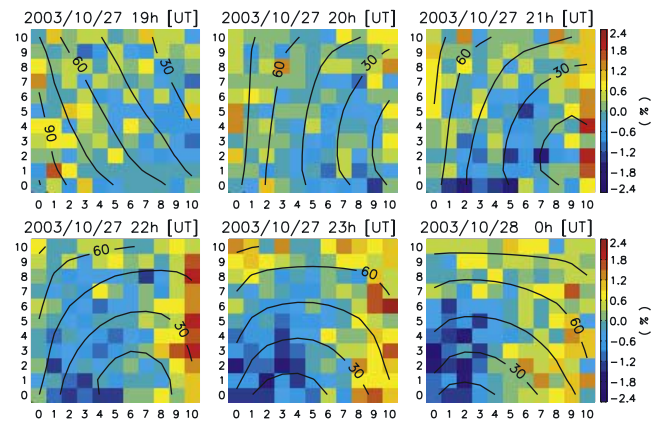
[7] Figure 2 shows $\Delta I_i^{obs}(t)$ in a 2D color contour format for 6 hours when the LC precursor is seen in Figure 1. Also shown in this plot is the contour line of the pitch angle calculated for cosmic rays incident to each directional channel with the median primary energy appropriate to that channel. It is seen in these 2D plots that the deficit intensity (displayed by blue color) is localized around small pitch angles. In the next section, we analyze the pitch angle distribution in space responsible for this LC precursor and make a quantitative comparison with the numerical results presented by paper 1.

3. Analysis and Results

[8] Following numerical simulations of LC precursors in paper 1, we model the pitch angle distribution of cosmic rays in space by a Gaussian function, as

$$f(\theta, P, \tau) = C_0 \left(\frac{P}{30}\right)^{-1} \exp\left(\frac{\tau}{T_0(P/30)^\gamma}\right) \exp\left(-\frac{\theta^2}{2\theta_0^2}\right) \quad (3)$$

where θ is the pitch angle measured from the sunward IMF, *P* is cosmic ray rigidity in GV, τ(<0) is the time in hour measured from the SSC onset time, T_0 is a free parameter denoting the lead-time (in hours) of LC precursor for 30 GV particles and C_0(<0) is a parameter describing the maximum intensity depression for 30 GV particles at τ = 0 and θ = 0°. We take 30 GV as the typical rigidity of primary cosmic rays modulated in FD and producing the secondary muons. The 1/*P* dependence of LC amplitude on *P* in equation (3) is assumed to follow the average dependence of the size of FD on particle rigidity. The additional two parameters, γ and θ_0,

Figure 2. The intensity distributions observed in 121 directional channels over 6 hours preceding the SSC. Each panel shows the hourly distribution of muon intensity in a 2D color contour format. Blue color denotes lower intensity. The vertical axis in each panel denotes the latitude of incident direction spanning from the north (upper) and south (lower) directions in the field of view, while the horizontal axis represents the longitude from the east (right) and west (left) directions. The pitch-angle measured from the observed IMF direction is shown by contour lines. The time (hour in universal time) indicated above each hourly map represents the start time of the corresponding hour.

Table 1. Best Fit Parameters for LC Precursor Observed on October 27–28, 2003[a]

$C_0[\%]$	$T_0[\text{hour}]$	$\theta_0[°]$	$\theta_{HW}[°]$	γ	S
−8.397	4.9	55	49.1	0.15	1.147

[a]Also shown is the "half-width" opening angle (θ_{HW}) calculated from θ_0 (see the next section in the text).

respectively represent the rigidity dependence of the lead-time and the opening angle of the LC.

[9] On the basis of numerical simulations, paper 1 quantitatively related the lead-time ($T_0(P/30)^\gamma$) and θ_{HW}; the "half-width" opening angle of LC, with physical parameters in interplanetary space, such as the "local" slope of the power spectrum of IMF turbulence (q), the parallel mean free path of the pitch angle scattering of cosmic rays (λ) and the angle between the IMF and the shock normal (θ_{Bn}). By using f defined in (3), we calculate the expected intensity $\Delta I_i^{cal}(\tau)$ for i-th directional channel, as

$$\Delta I_i^{cal}(\tau) = I_i^{cal}(\tau) - \overline{I^{cal}}(\tau), \qquad (4)$$

where

$$I_i^{cal}(\tau) = \frac{\int_{P_i^{cut}}^\infty N_i(P)f(\theta_i(\tau,P),P,\tau)dP}{\int_{P_i^{cut}}^\infty N_i(P)dP} \qquad (5)$$

and

$$\overline{I^{cal}}(\tau) = \frac{1}{121}\sum_{i=1}^{121} I_i^{cal}(\tau). \qquad (6)$$

In (5), $N_i(P)$, representing the number of muons produced by primary particles with rigidity P and recorded in i-th channel, is calculated by utilizing the response function of muons in the atmosphere to primary particles [*Murakami et al.*, 1979]. P_i^{cut} represents the minimum (cut-off) rigidity of primary cosmic rays to produce muons recorded in i-th channel. By repeating the calculation of $\Delta I_i^{cal}(\tau)$ in (4) for various sets of free parameters, C_0, γ, T_0 and θ_0, we determine the best fit set for n-hours which minimizes S defined as

$$S = \sqrt{\frac{1}{n}\sum_{j=1}^{n} s^2(\tau_j)}, \qquad (7)$$
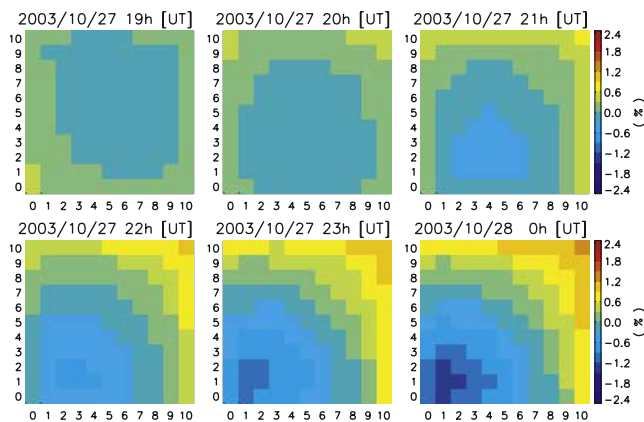
where

$$s(\tau_j) = \sqrt{\frac{1}{121}\sum_{i=1}^{121} \frac{\left(\Delta I_i^{obs}(\tau_j) - \Delta I_i^{cal}(\tau_j)\right)^2}{\sigma_i^2}}, \qquad (8)$$

and σ_i is the error deduced from the average hourly count rate of muons in the i-th channel. Note that C_0 can be uniquely determined for each set of γ, T_0 and θ_0. We repeat this best fit calculation by changing the fitting period n from 7 hours to 12 hours preceding the SSC, until the best fit parameters converge well. We exclude from the best fit computation the hour immediately before the SSC, because the LC center left the field of view by this time.

[10] Table 1 shows the best fit parameters together with the average residual S in (7), while Figure 3 displays 2D color contours of $\Delta I_i^{cal}(\tau)$ reproduced with these parameters. Figure 3 displays a good resemblance to Figure 2 in each corresponding hour, suggesting that $\Delta I_i^{obs}(\tau)$ is well reproduced with the model distribution in (3). This is also confirmed in Figure 4 showing the scatterplot between $\Delta I_i^{obs}(\tau)$ and the best fit $\Delta I_i^{cal}(\tau)$. The regression and correlation coefficients in this figure are respectively 1.03 and 0.61.

[11] To examine whether the best fit parameters in Table 1 are consistent with $\Delta I_i^{obs}(\tau)$ for each τ, we also calculate the $\Delta I_i^{cal}(\tau)$ on hourly basis, substituting f in (3) with

$$f'(\theta,P,\tau) = C_0'(\tau)\left(\frac{P}{30}\right)^{-1}\exp\left(\frac{\tau}{T_0(P/30)^\gamma}\right)\exp\left(-\frac{\theta^2}{2\theta_0^2}\right) \qquad (9)$$

and determine $C_0'(\tau)$ which minimizes $s(\tau)$ in equation (8). In this calculation, we fix T_0, θ_0 and γ at the values in Table 1. Figure 5 displays the resulting $C_0'(\tau)\exp(\tau/T_0)$ representing the amplitude of LC at 30 GV in space as a function of τ. Also plotted in this figure is a curve representing $C_0\exp(\tau/T_0)$ with C_0 in Table 1. It is again seen that the parameters in Table 1 are consistent with $C_0'(\tau)$ obtained for each hour. Nevertheless $C_0'(\tau)\exp(\tau/T_0)$ scatters around the curve. In the next section, we will discuss the physical implications of the best fit parameters in Table 1, referring to theoretical results presented by paper 1.

4. Discussion and Conclusion

[12] The "half-width" opening angle θ_{HW} is defined in paper 1 as the pitch angle at which the intensity decrease

Figure 3. The intensity distributions reproduced from the best fit parameters in Table 1 and plotted in the same format as Figure 2.
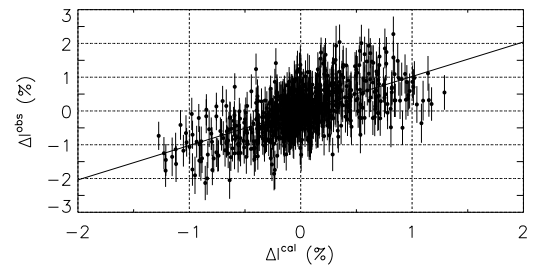
Figure 4. The scatterplot between ΔI^{obs} (ordinate) and the best fit ΔI^{cal} (abscissa) for 6 hours plotted in Figures 2 and 3. A total of 726 (= 6 × 121) data points are plotted in this figure.
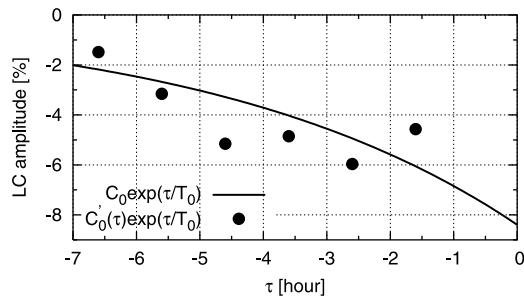
Figure 5. The best fit LC amplitude at 30 GV as a function of time (τ) measured from the SSC (solid curve). Also plotted are amplitudes derived from the best fitting on an hourly basis (see text).

(relative to the omnidirectional intensity) has reached half its maximum value. Taking into account the fact that omnidirectional intensity varies with time in equation (3), we determined that θ_{HW} is given by $0.893\theta_0 = 49.1°$ using the parameters given in Table 1. This θ_{HW} suggests that the LC in this event has a rather broad angular distribution in space. According to a numerical relationship between the loss cone width (θ_{HW}) and θ_{Bn}, $\theta_{HW} = 49.1°$ corresponds to $\theta_{Bn} \sim 6°$ assuming $q = 0.5$, which implies that the shock in this event is a "quasi parallel" shock (see Figure 7 in paper 1).

[13] On the other hand, using in situ IMF and plasma data we obtain $\theta_{Bn} \sim 60°$ from the coplanarity condition. This appears consistent with an "Alaska model" simulation (http://gse.gi.alaska.edu/). The parent event was either an X1.2 flare (N02W38) at 17:21 UT or another X1.2 flare (S15E44) at 05:57 UT (and/or the associated CMEs) on 26 October 2003 (ftp://ftp.ngdc.noaa.gov/STP/SOLAR_DATA/SOLAR_FLARES/XRAY_FLARES/).

[14] The shock normal angle derived from the loss cone appears to be in conflict with that derived from in situ measurements. We are aware of three possible sources for this seeming conflict. First, the "Alaska model" simulation indicates that a large shock was overtaking a smaller shock westward of Earth. During the loss cone period, Earth may have been connected with the westward shock which is more consistent with a quasi-parallel geometry. Second, there is evidence from multi-spacecraft measurements [*Szabo et al.*, 2001] that interplanetary shocks have a corrugated surface, such that relatively close spacecraft report significantly different shock normal angles. In contrast, the shock normal reported here presumably reflects the large-scale structure of the shock, as it is based upon particles with large Larmor radii (~ 0.1 AU). Third, it is possible that our current analysis method overestimates the loss cone opening angle, because we neglect (at present) the finite aperture angle of each directional channel, which is about 15 degree for the vertical channel. In reality, there is a spread of directions from the different angles of incidence in each channel, and this spread may contribute a spurious addition to the computed value of θ_0.

[15] The derived lead-time T_0 for 30 GV particles in Table 1 corresponds to the "decay length" l of the LC, as

$$l = T_0 V_s / \cos\theta_{Bn} \sim 0.053\, AU \qquad (10)$$

with $\theta_{Bn} = 6°$ and the average solar wind velocity of $V_s = 450$ km/s over the period analyzed (see Figure 1). By using a ratio $l/\lambda = 0.082$ derived for $q = 0.5$ and $\theta_{HW} = 49.1°$ from interpolating values in Table 2 in paper 1, we estimate the parallel mean free path for interplanetary scattering (λ) to be ~ 0.65 AU, 2 times shorter than 1.5 AU estimated by paper 1 for the muon detector. This implies that the IMF is more turbulent in this event than a typical power spectrum assumed in paper 1. These conclusions with $q = 0.5$ remain unchanged even if we choose $q = 1.0$, with which we get $\theta_{Bn} \sim 12°$, $l \sim 0.054\, AU$ and $\lambda \sim 0.56\, AU$.

[16] The derived rigidity dependence of the lead-time $((P/30)^{0.15})$ in Table 1, on the other hand, suggests that the lead-time of this LC at neutron monitor energy (10 GV) is $T_0(1/3)^{0.15} \sim 4.2$ hours remaining similar to T_0 in Table 1. This implies that this LC could be observed by the neutron monitor on an hourly basis. This is consistent with a LC signature also seen in the hourly count rate recorded by a neutron monitor at Mt. Norikura.

References

Fujimoto, K., et al. (2001), Observation of forbush decrease by the narrow angle muon telescope at Mt. Norikura, paper presented at 27th International Cosmic Ray Conference, Copernicus Ges., Hamburg, Germany.

Fujimoto, K., et al. (2003), Observation of precursory decrease by the narrow angle muon telescope at Mt. Norikura, paper presented at 28th International Cosmic Ray Conference, Inst. for Cosmic Ray Res., Univ. of Tokyo, Tsukuba, Japan.

Kuwabara, T., et al. (2004), Geometry of an interplanetary CME on October 29, 2003 deduced from cosmic rays, *Geophys. Res. Lett.*, *31*, L19803, doi:10.1029/2004GL020803.

Leerungnavarat, K., et al. (2003), Loss cone precursors to forbush decreases and advance warning of space weather effects, *Astrophys. J.*, *593*, 587–596.

Munakata, K., J. W. Bieber, S. Yasue, C. Kato, M. Koyama, S. Akahane, K. Fujimoto, Z. Fujii, J. E. Humble, and M. L. Duldig (2000), Precursors of geomagnetic storms observed by the muon detector network, *J. Geophys. Res.*, *105*, 27,457–27,468.

Murakami, K., et al. (1979), Response functions for cosmic-ray muons at various depths underground, *Nuovo Cimento Soc. Ital. Fis. C*, *2*, 635–651.

Ohashi, Y., et al. (1997), New narrow angle muon telescope at Mt. Norikura, paper presented at 25th International Cosmic Ray Conference, Durban, Int. Union of Pure and Appl. Phys., South Africa.

Sagisaka, S. (1986), Atmospheric effects on comic-ray muon intensities at deep underground depth, *Nuovo Cimento Soc. Ital. Fis. C*, *9*, 809–828.

Szabo, A., R. P. Lepping, J. Merka, C. W. Smith, and R. M. Skoug (2001), The evolution of interplanetary shocks driven by magnetic clouds, in *Solar Encounter: Proceedings of the First Solar Orbiter Workshop*, edited by B. Battrick and H. Sawaya-Lacoste, *Eur. Space Agency Spec. Publ.*, ESA SP-493, 383–387.

———————————
S. Akahane, C. Kato, M. Koyama, T. Kuwabara, K. Munakata, and S. Yasue, Physics Department, Shinshu University, Matsumoto 390-8621, Japan. (kmuna00@gipac.shinshu-u.ac.jp)

T. Aoki, Y. Ohashi, and A. Okada, Institute for Cosmic Ray Research, University of Tokyo, Kashiwa 277-8582, Japan.

J. W. Bieber, Bartol Research Institute, University of Delaware, Newark, DE 19716, USA. (john@bartol.udel.edu)

H. Kojima, Faculty of Domestic Science, Nagoya Women's University, Nagoya 467-8610, Japan.

K. Mitsui, Faculty of Management Information, Yamanashi Gakuin University, Kofu 400-8575, Japan.